A comprehensive design and rating study of evaporative coolers and condensers. Part II. Sensitivity analysis

Bilal A. Qureshi, Syed M. Zubair*

Mechanical Engineering Department, King Fahd University of Petroleum and Minerals, KFUPM Box #1474, Dhahran 31261, Saudi Arabia

Abstract

Sensitivity analysis can be used to identify important model parameters, in particular, normalized sensitivity coefficients; by allowing a one-on-one comparison. Regarding design of evaporative coolers, the sensitivity analysis shows that all sensitivities are unaffected by varying the mass flow ratio and that outlet process fluid temperature is the most important factor. In rating evaporative coolers, effectiveness is found to be most sensitive to the process fluid flow rate. Also, the process fluid outlet temperature is most sensitive to the process fluid inlet temperature. For evaporative condensers, the normalized sensitivity coefficient values indicate that the condensing temperature is the most sensitive parameter and that these are not affected by the value of the mass flow ratio. For evaporative condenser design, it was seen that, for a 53% increase in the inlet relative humidity, the normalized sensitivity of the surface area increased 1.8 times in value and, for a 15 °C increase in the condenser temperature, the sensitivity increased by 3.5 times. The performance study of evaporative condensers show that, for a 72% increase in the inlet relative humidity, the normalized sensitivity coefficient for effectiveness increased 2.4 times and, for a 15 °C increase in the condenser temperature, it doubled in value.
© 2005 Elsevier Ltd and IIR. All rights reserved.

Keywords: Refrigeration; Air conditioning; Cooling tower; Evaporative condenser; Modelling; Research; Parameter

Etude approfondie et évaluation des tours de refroidissement et condenseurs évaporatifs. Partie II. Analyse de la sensibilité

Mots clés : Froid; Conditionnement d'air; Tour de refroidissement; Condenseur évaporatif; Modélisation; Recherche; Paramétre

1. On sensitivity analysis

Sensitivity analysis is a means to acquire insight about the importance of model parameters and, in turn, identify those, which are more responsive. Kitchell et al. [1] further

explain that sensitivity analysis results are used to identify the most important model parameters, areas for future research, and the level of precision required for measuring system input variables. Masi et al. [2] clarified that, as a general rule, local methods require less extensive calculations, and provide a higher level of detail, whereas global methods may be best for handling large variations in the system parameters. In general, sensitivity analysis involves making changes to model rate coefficients singly or in

* Corresponding author. Tel.: +966 3 860 3135; fax: +966 3 860 2949.

E-mail address: smzubair@kfupm.edu.sa (S.M. Zubair).

Nomenclature

A	outside surface area of cooling tubes (m^2)
Le	Lewis number ($Le = h_c/h_D c_{p,a}$)
$\dot{m}$	mass flow rate of fluid (kg s^{-1})
m_{ratio}	water-to-air mass flow rate ratio ($m_{ratio} = \dot{m}_{w,in}/\dot{m}_a$)
NSC	normalized sensitivity coefficient
NTU	number of transfer units
NU	normalized uncertainty
SA	sensitivity analysis
t	temperature (°C)
U_Y	uncertainty in parameter Y, units of Y
U_{X_i}	uncertainty in parameter X_i, units of X_i
w.r.t.	with respect to
$\bar{X}$	nominal value of X, units of X
X_i	general input variable

Y	response parameter
$\bar{Y}$	nominal value of Y, units of Y
ε	effectiveness
$\in$	represents the perturbation value, units of X_i

Subscripts

a	air
ec	evaporative condenser
efc	evaporative fluid cooler
in	inlet
N	maximum number of independent variables
out	outlet
p	process fluid
r	refrigerant
wb	wet-bulb

---

combinations and determining the resulting changes in the model output [3]. In other words, sensitivities reflect the change rates (derivatives) of system responses with respect to design variables [4,5]. It should be noted that the aim of sensitivity analysis is to allow the comparison, on a common basis, of the role of different process parameters. The use of the normalized sensitivity coefficients, in particular, allows the direct comparison of parameters whose order of magnitude could be significantly different.

For instance, any independent variable X can be represented as

$$X = \bar{X} \pm U_X \tag{1}$$

where $\bar{X}$ denotes its nominal value and U_X its uncertainty about the nominal value. The $\pm U_X$ interval is defined as the band within which the true value of the variable X can be expected to lie with a certain level of confidence (typically 95%) [6]. In general, if a function $Y(X)$ represents an output parameter, then the uncertainty in Y due to an uncertainty in X can be expressed as

$$U_Y = \frac{dY}{dX} U_X \tag{2}$$

It is important to note that the uncertainty in a computed result could be estimated with good accuracy using a root-sum-square combination of the effects of each of the individual inputs. For a multivariable function $Y = Y(X_1, X_2, X_3 \ldots, X_N)$, the uncertainty in Y due to uncertainties in the independent variables is given by the root sum square product of the individual uncertainties computed to first order accuracy as [7,8]

$$U_Y = \left[\sum_{i=1}^{N} \left(\frac{\partial Y}{\partial X_i} U_{X_i} \right)^2 \right]^{1/2} \tag{3}$$

Physically, each partial derivative in the above equation represents the sensitivity of the parameter Y to small

changes in the independent variable X_i. We note that the partial derivatives are typically defined as the sensitivity coefficients.

By normalizing the uncertainties in the response parameter Y and the various input variables by their respective nominal values, Eq. (3) can be written as

$$\left(\frac{U_Y}{\bar{Y}} \right) = \left\{ \sum_{i=1}^{N} \left[\left(\frac{\partial Y}{\partial \bar{Y}} \frac{\bar{X}_i}{\partial X_i} \right) \left(\frac{U_{X_i}}{\bar{X}_i} \right) \right]^2 \right\}^{1/2} \tag{4}$$

The dimensionless terms in braces on the right hand side of the above equation represent the respective sensitivity coefficients and uncertainties in their normalized forms and are, therefore, referred to as normalized sensitivity coefficients (NSCs) and normalized uncertainties (NUs) [5]. Eq. (4) can, therefore, be written as

$$\left(\frac{U_Y}{\bar{Y}} \right) = \left\{ \sum_{i=1}^{N} \left[NSC_{X_i} NU_{X_i} \right] \right\}^{1/2} \tag{5}$$

Currently, only NSC is of interest to us. On replacing partial derivatives by ratios of discrete changes, the normalized sensitivity coefficients can be expressed as

$$NSC_{X_i} = \left(\frac{\Delta Y_i}{\bar{Y}} \frac{\bar{X}_i}{\Delta X_i} \right)^2 \tag{6}$$

Since the sensitivity coefficients of the various input variables are normalized relative to the same nominal value $\bar{Y}$, a one-on-one comparison of the coefficients can be made thereby yielding a good estimate of the sensitivity of the result to each of the variables. Masi et al. [2] explained that the practical meaning of the normalized sensitivity coefficient is to establish how many order of magnitude of variation should be expected for the analyzed function when the considered parameter is altered by one order of magnitude. Obviously, a one order of magnitude alteration is usually not of practical interest, and it should be viewed

only as a limiting situation to obtain directly comparable values.

It is thus important to note that the normalized sensitivity coefficients are obtained as a significant characteristic parameter since these coefficients identify the input variables to which the performance parameters are most sensitive, irrespective of the uncertainty in the input variables themselves [9]. Masi et al. [2] stated that the advantage of applying the sensitivity analysis using validated models instead of using directly experimental information is due to the possibility to isolate single answers to single perturbation of a process parameter. This performance is hard to obtain experimentally being the process parameters strictly correlated. Guo and Zhao [10] showed, through numerical analysis of an indirect evaporative air cooler, that a higher effectiveness is achieved for a smaller channel width, a lower inlet relative humidity of the secondary air stream, a higher wettability of the plate and a higher velocity ratio of the secondary air to the primary air stream. Zalewski et al. [11], however, attempted the optimization of the geometrical and operating parameters of an evaporative fluid cooler to ensure minimum cost using sensitivity coefficients that were not normalized.

The objective of this paper is to carry out a sensitivity analysis, employing normalized sensitivity coefficients, for evaporative coolers and evaporative condensers. In this regard, the effect of contributing input variables that influence the sensitivity of the response variables of these systems are investigated using the mathematical models based on Dreyer [12]. First, we briefly describe the method that is used to calculate the normalized sensitivity coefficients.

2. Solution procedure

The engineering equation solver (EES) program was used to generate the necessary numerical values required to perform the sensitivity analysis. In this regard, the response variables for the sensitivity analysis were selected to reflect the objectives of this paper as well as to their utility in aiding the interpretation of the sensitivity analysis results. The analysis can be accomplished by the method of sequential perturbation, shown schematically in Fig. 1(a) and (b) and detailed as follows [13]:

- Calculate the result Y from the data $(\bar{X}_{i...N})$ and designate it as the nominal value $\bar{Y}$.
- Increase the value of the ith variable by its interval (U_{X_i}) and calculate the response variable with all others at their nominal values. Record the value of ith variable as X_{i+} and the result as Y_{i+}. Similarly, calculate Y_{i-} at X_{i-} as a result of decreasing the ith variable by its interval.
- Then let $\Delta Y_i = |Y_{i+} - Y_{i-}|$ and similarly $\Delta X_i = |X_{i+} - X_{i-}|$.
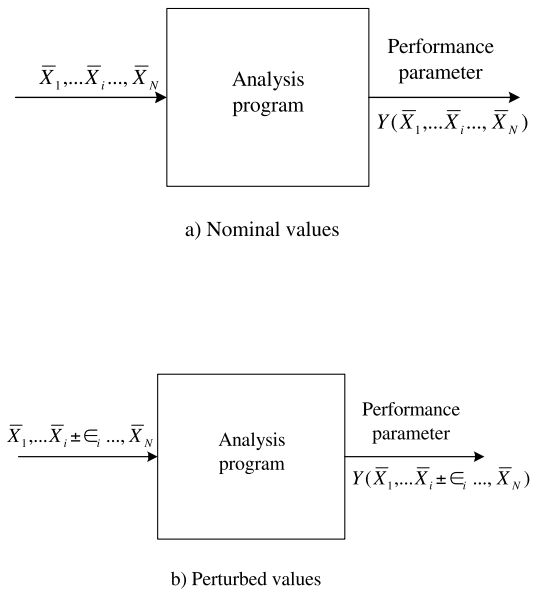

a) Nominal values

b) Perturbed values

Fig. 1. Block diagram of sensitivity analysis procedure: (a) nominal values; and (b) perturbed values.

- Calculate the required NSC of the ith variable (X_i) by plugging in the calculated values in Eq. (6).

It is noted that this method is similar to the one proposed by James et al. [9]. Sensitivity analysis can be applied with either arbitrarily selected ranges of variation or variations that represent known ranges of uncertainty [14]. The perturbation selected was $\pm 1\,°C$ (representative) for the temperatures and 10% (arbitrary) of the original value for the flow rates.

A numerical example is shown below for a single value calculated at an inlet wet-bulb temperature of 12.11 °C (refer to Fig. 2(a)) where the process fluid outlet temperature is considered as the independent variable ($X_i = t_{p,out}$) and the response variable is chosen to be the required surface area of the tubes ($Y = A$). We follow the following steps to get the sensitivity coefficients:

Step (a): For a process fluid outlet temperature of 42.69 °C, the required surface area is found to be 1.598 m². Therefore, $\bar{t}_{p,out} = 42.69\,°C$ and $\bar{A} = 1.598\,m^2$.

Step (b): When the process fluid outlet temperature is increased by 1 °C, the resulting area is 1.281 m². Therefore, $t_{p,out+} = 43.69\,°C$ and $A_+ = 1.281\,m^2$. Similarly, with $t_{p,out-} = 41.69\,°C$, the required surface is calculated as $A_- = 1.979\,m^2$.

Step (c): Thus, we find that $\Delta t_{p,out} = 2\,°C$ and $\Delta A = 0.698\,m^2$.

Step (d): Substituting all the necessary values in Eq. (6), we get the NSC value as 87, which is seen as a plotted value in Fig. 2(a).

It should be noted that the symbolism used in the y-axis of Figs. 2–11 follows the format NSC (response variable,

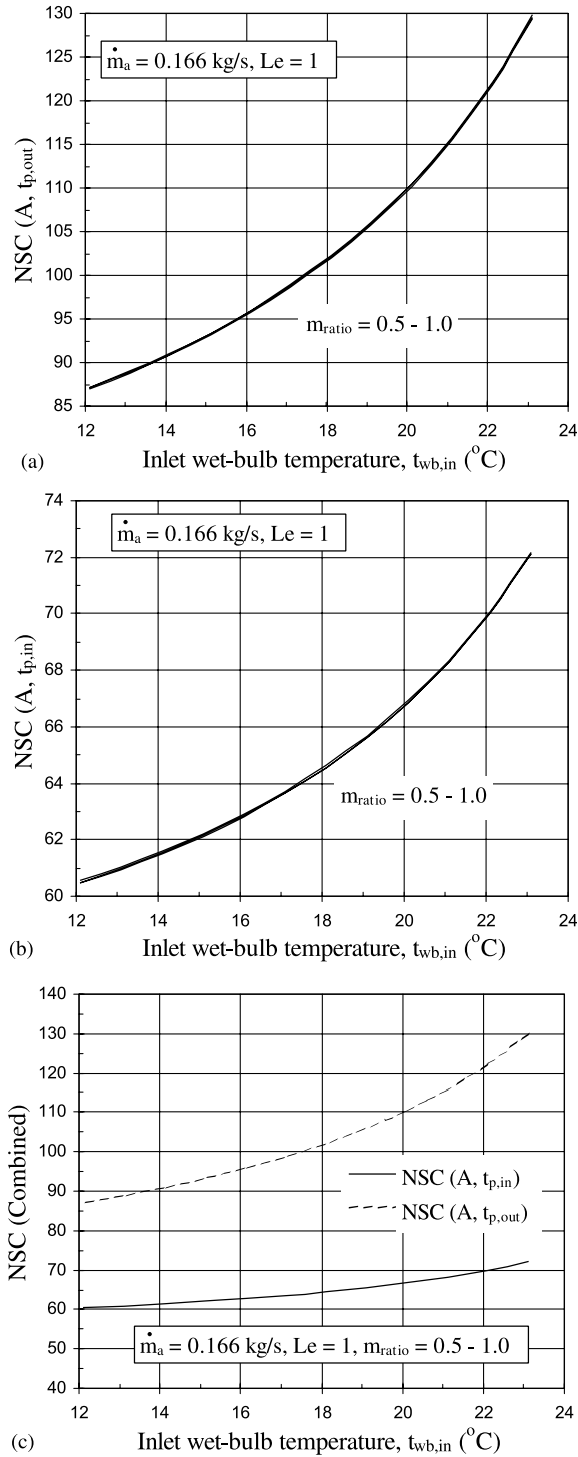Fig. 2. Variation of area NSC as a function of $t_{wb,in}$ and different mass flow rate ratios; (a) with respect to $t_{p,out}$; (b) with respect to $t_{p,in}$; and (c) combined.

independent variable) wherein the latter in brackets is the variable that is perturbed.

The limits of the various variables used in the next section can be seen in Table 1. It should be noted that the inlet wet bulb temperature ($t_{wb,in}$) and water to air flow ratio ($m_{ratio} = \dot{m}_{w,in}/\dot{m}_a$) is varied identically in both the evaporative cooler and condenser. The effectiveness of the evaporative fluid cooler and condenser are defined as the ratio of actual energy to the maximum possible energy transfer from the fluid in the tubes and are given by [15]

$$\varepsilon_{efc} = \frac{t_{p,in} - t_{p,out}}{t_{p,in} - t_{wb,in}}; \quad \varepsilon_{ec} = \frac{h_{r,in} - h_{r,out}}{h_{r,in} - h_{wb,in}} \quad (7)$$

3. Sensitivity analysis—evaporative fluid cooler

The computer model of the evaporative cooler described in Dreyer [12] and the companion paper [15] is used to carry out the sensitivity analysis by following the procedure described above. Initial tests that included various parameters such as all mass flow rates (air, water and process fluid) and relevant (ambient and process fluid) temperatures showed that the outlet process fluid temperature ($t_{p,out}$) and the inlet process fluid temperature ($t_{p,in}$) had the largest comparable values of the normalized sensitivity coefficients where design is concerned but, in rating, the process fluid flow rate ($\dot{m}_p$) and the inlet process fluid temperature ($t_{p,in}$) had the highest comparable values. Therefore, variation in the sensitivity values of only these coefficients was shown.

3.1. Design study

Fig. 2(a) and (b) are normalized forms of the plots between (surface) area sensitivity coefficients ($\partial A/\partial t_{p,out}$) and ($\partial A/\partial t_{p,in}$) versus the inlet wet-bulb temperature ($t_{wb,in}$), for different values of mass flow rate ratio (m_{ratio}). These figures show that, as the value of the inlet wet bulb temperature increases, the sensitivities in both cases increase in a very similar manner. The effect of mass flow rate ratio is negligible. In the former, as the inlet wet-bulb temperature ($t_{wb,in}$) increases, the decreasing difference between the outlet process fluid temperature ($t_{p,out}$) and the

Table 1
A summary table with the numeric limits of various variables

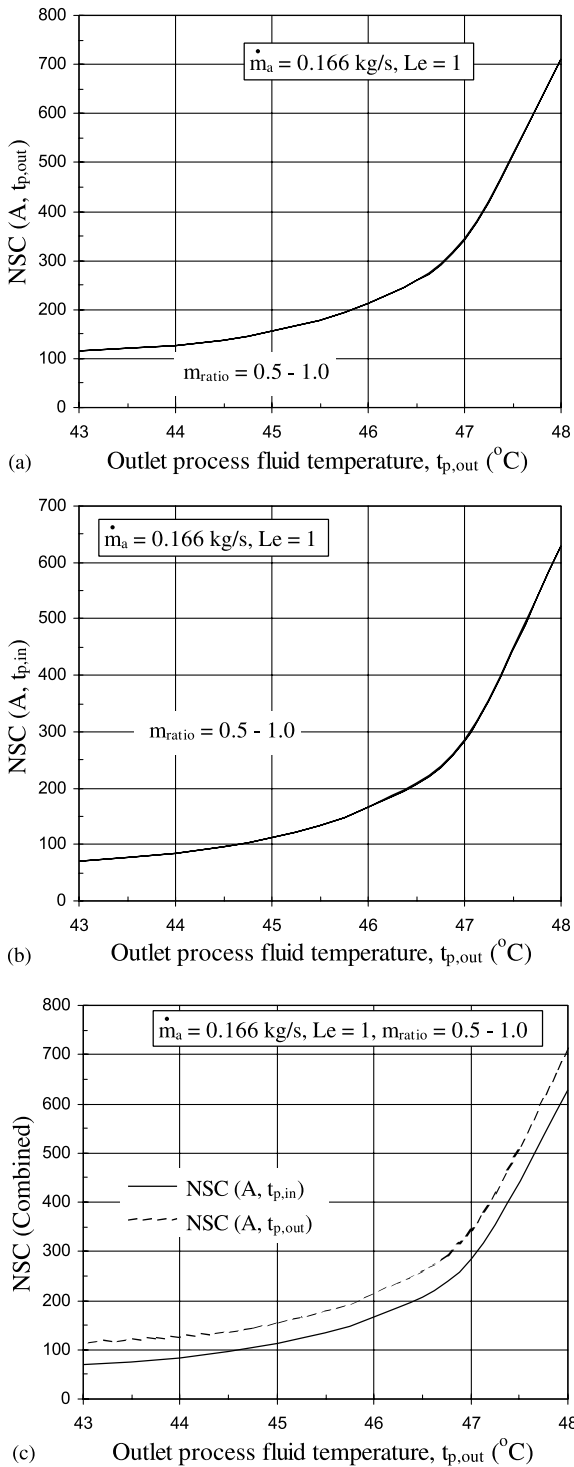|	Design	Rating
Inlet wet-bulb temperature ($t_{wb,in}$)	12.11–23.11	12.11–26.11
Outlet process fluid temperature ($t_{p,out}$)	43–48	–
Inlet process fluid temperature ($t_{p,in}$)	–	40–60
Condensing temperature (t_r)	35–50	35–50
Mass flow rate ratio	0.5, 0.75, 1	0.5, 0.75, 1

Fig. 3. Variation of area NSC as a function of $t_{p,out}$ and different mass flow rate ratios; (a) with respect to $t_{p,out}$; (b) with respect to $t_{p,in}$; and (c) combined.

inlet wet-bulb temperature ($t_{wb,in}$) gives rise to larger surface area requirements as well as a higher rate of the change of the same as the outlet process fluid temperature ($t_{p,out}$) is constant. Mass flow rate ratio has a negligible effect as, with the inlet and outlet process fluid temperatures fixed, it mainly affects the steady-state water temperature, which subsequently changes the amount of water evaporated. Similarly, in Fig. 2(b), the sensitivity increases with an increase in the inlet wet-bulb temperature ($t_{wb,in}$) with mass flow rate ratios having a negligible effect. With the inlet process fluid temperature ($t_{p,in}$), its perturbation ($\Delta t_{p,in}$) as well as the outlet process fluid temperature ($t_{p,out}$) constant, the area as well as resulting changes in area (ΔA) (due to the perturbation in the inlet process fluid temperature) increase, which combine to increase the NSC. It should be kept in mind that the increase in area and negligible effect of mass flow rate ratio is due to the same reasons as explained for the previous figure. Fig. 2(c) combines these NSCs illustrating their variation with respect to each other and clearly indicating that the area NSC with respect to process fluid outlet temperature dominates at all mass flow ratios. It is also noted that the ratio NSC(A, $t_{p,out}$)/NSC(A, $t_{p,in}$) is in the range of 1.44–1.8.

Fig. 3(a) and (b) are normalized forms of the plots between (surface) area sensitivity coefficients ($\partial A/\partial t_{p,out}$) and ($\partial A/\partial t_{p,in}$) versus the process fluid outlet temperature ($t_{p,out}$), for different values of mass flow rate ratio. Fig. 3(a) and (b) show that, as the value of the process fluid outlet temperature increases, the sensitivities in both cases increase in a very similar manner with the effect of mass flow rate ratio being negligible. In Fig. 3(a), as the outlet process fluid temperature ($t_{p,out}$) increases, the decreasing difference between the outlet process fluid temperature ($t_{p,out}$) and the inlet process fluid temperature ($t_{p,in}$) gives rise to smaller surface area requirements as well as a lower rate of the change of the same. It was noted that the perturbation ($\Delta t_{p,in}$) is constant and all these factors combine to increase the NSC where it's very high final value is due to the very small value of ($t_{p,in} - t_{p,out}$). Mass flow rate ratio has a minor effect as it mainly changes the steady-state water temperature. Fig. 3(b) is different from Fig. 3(a) in this respect that, both, the inlet process fluid temperature ($t_{p,in}$) and its perturbation ($\Delta t_{p,in}$), are constant and these factors combine to increase the NSC as the process fluid outlet temperature ($t_{p,out}$) increases where, again, its very high final value is due to the very small value of ($t_{p,in} - t_{p,out}$). Fig. 3(c) shows that the NSCs increase, in both cases, as the inlet process fluid temperature ($t_{p,in}$) increases and reaches a minimum around 43 °C with the NSC with respect to the outlet process fluid temperature ($t_{p,out}$) always higher. Finally, it is also seen that the ratio NSC(A, $t_{p,out}$)/NSC(A, $t_{p,in}$) is in the range of 1.64–1.13.

3.2. Rating study

Fig. 4(a) and (b) are normalized forms of the plots between effectiveness sensitivity coefficients ($\partial \varepsilon_{efc}/\partial t_{p,in}$)

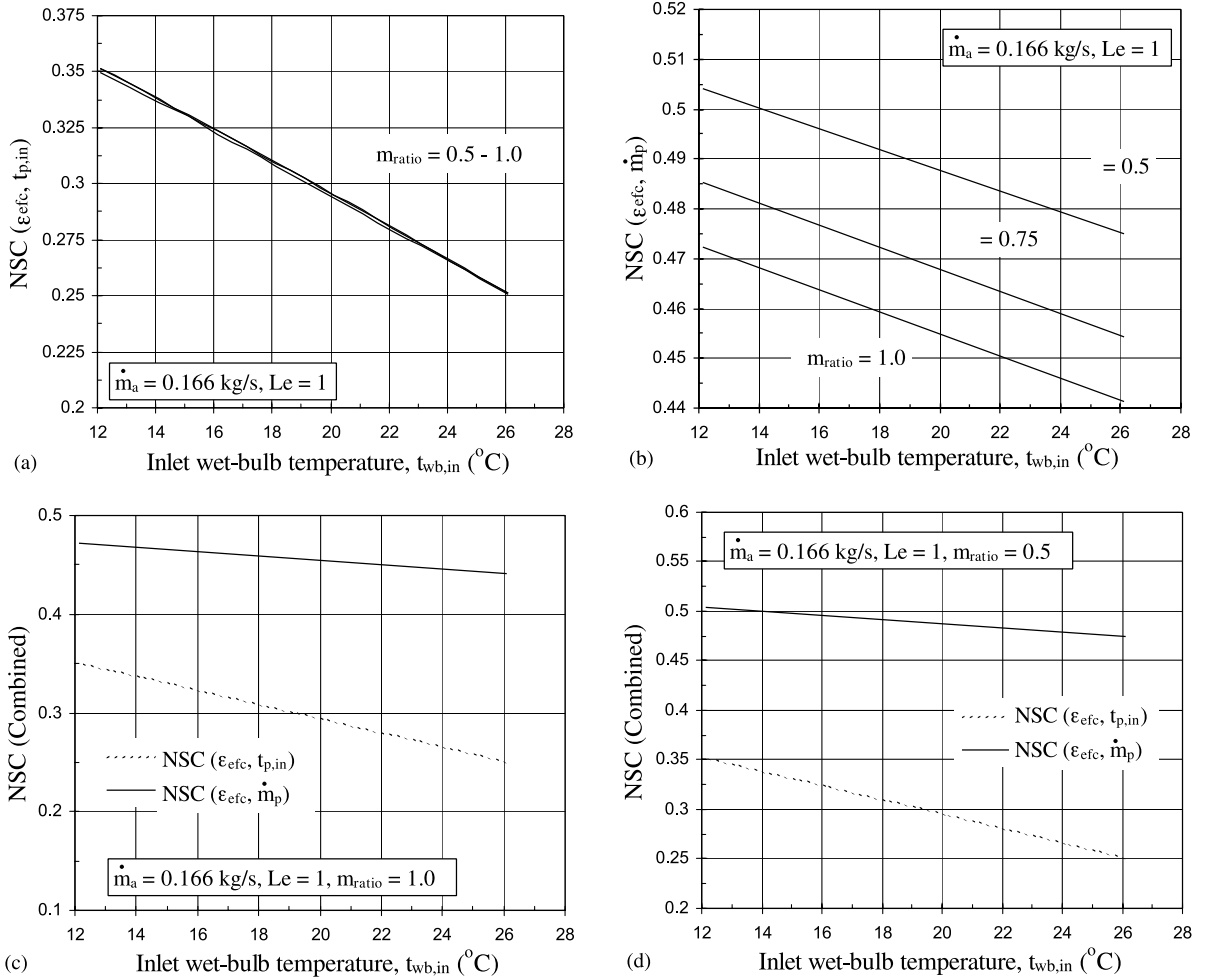Fig. 4. Variation of effectiveness NSC as a function of $t_{wb,in}$ and different mass flow rate ratios; (a) with respect to $t_{p,in}$; (b) with respect to $\dot{m}_p$; (c) combined for $m_{ratio} = 1.0$; and (d) combined for $m_{ratio} = 0.5$.

and $(\partial\varepsilon_{efc}/\partial\dot{m}_p)$ versus the inlet wet-bulb temperature $(t_{wb,in})$, for different mass flow rate ratios. These figures show that, as the inlet wet-bulb temperature decreases, the sensitivity of the effectiveness with respect to the inlet process fluid temperature $(t_{p,in})$ and the process fluid flow rate $(\dot{m}_p)$ increases. In the latter case, the NSC is lower for large mass flow rate ratios but remains virtually unchanged in case of the former. In Fig. 4(a), as the inlet wet-bulb temperature $(t_{wb,in})$ increases, the effectiveness increases due to the decreasing difference between the outlet process fluid temperature $(t_{p,out})$ and the inlet wet-bulb temperature $(t_{wb,in})$ keeping in mind that the surface area is constant. With the inlet process fluid temperature $(t_{p,in})$ as well its perturbation $(\Delta t_{p,in})$ constant and the effectiveness increasing with the rising wet-bulb temperature, the combination of these quantities causes the NSC to decrease. Mass flow rate ratio has a small effect as most of the effect is compensated by a change in the steady-state water temperature, which

subsequently changes the amount of water evaporated. In Fig. 4(b) as well, the increasing wet-bulb temperature, increases the effectiveness due to the same reasons as explained before. With the process fluid flow rate $(\dot{m}_p)$ as well its perturbation $(\Delta\dot{m}_p)$ constant and the effectiveness a well as the resulting changes in it $(\Delta\varepsilon_{efc})$ increasing with the rising wet-bulb temperature, the combination of these quantities causes the NSC to decrease. At a comparatively lower mass flow ratio, effectiveness as well as changes in it $(\Delta\varepsilon_{efc})$ is smaller and, thus, NSC is higher. The lower effectiveness is due to the higher steady-state water temperature achieved that causes less heat transfer. Although this is also true for Fig. 4(a) as well, the effect is more significant with respect to the process fluid flow rate as the system is more sensitive to this factor, which is evident from Fig. 4(c) and (d) where these two NSCs are combined.

Similarly, Fig. 5(a) and (b) are normalized forms of the plots between effectiveness sensitivity coefficients $(\partial\varepsilon_{efc}/$
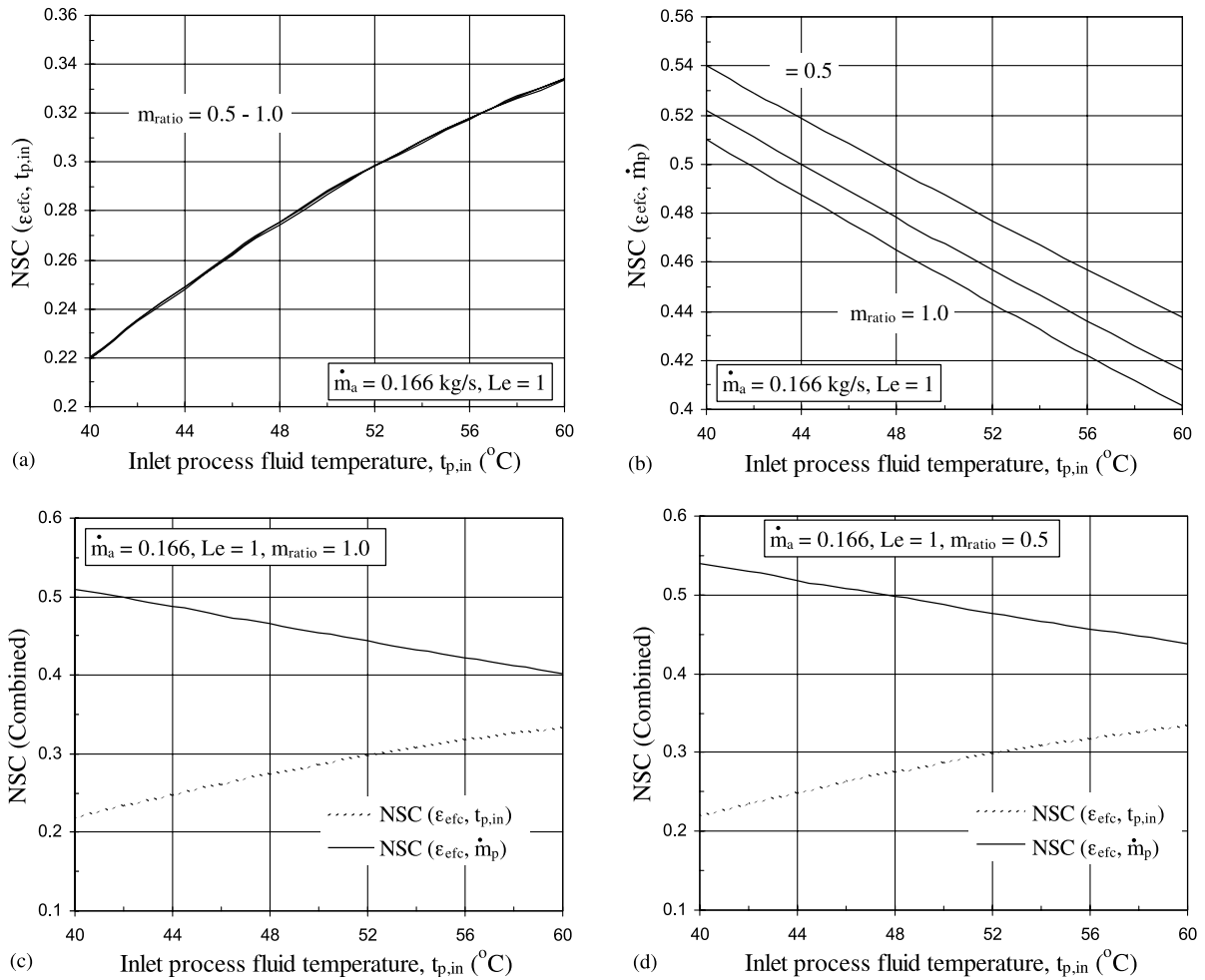
Fig. 5. Variation of effectiveness NSC as a function of $t_{p,in}$ and different mass flow rate ratios; (a) with respect to $t_{p,in}$; (b) with respect to $\dot{m}_p$; (c) combined for $m_{ratio} = 1.0$; and (d) combined for $m_{ratio} = 0.5$.

$\partial t_{p,in}$) and ($\partial \varepsilon_{efc} / \partial \dot{m}_p$) versus the inlet process fluid temperature ($t_{p,in}$), for different mass flow rate ratios. Fig. 5(a) shows that as the inlet process fluid temperature ($t_{p,in}$) increases, the NSC with respect to the inlet process fluid temperature ($t_{p,in}$) also increases and there is little effect of mass flow rate ratio. Also, the effectiveness increases due to the increasing difference between the inlet process fluid temperature ($t_{p,in}$) and the outlet process fluid temperature ($t_{p,out}$) keeping in mind that the surface area is constant. Now, with effectiveness (ε_{efc}) and the inlet process fluid temperature ($t_{p,in}$) increasing and the perturbation of the latter ($\Delta t_{p,in}$) constant, the combination of these quantities causes the NSC to increase as the process fluid inlet temperature increases at a much faster rate than the effectiveness. In Fig. 5(b) as well, the increasing inlet process fluid temperature increases the effectiveness due to the same reasons as explained before. The NSC with respect to the process fluid mass flow rate decreases due to the

reasons described earlier for Fig. 4(b). Also, differences seen in NSC values due to varying mass flow ratios is due to a similar explanation as mentioned for Fig. 4(b). Fig. 5(c) and (d) combine these two NSCs to show that thermal effectiveness is more sensitive to the process fluid flow rate ($\dot{m}_p$).

Fig. 6 is the normalized form of the plot between process fluid outlet temperature sensitivity coefficient ($\partial t_{p,out} / \partial t_{p,in}$) versus the inlet wet-bulb temperature ($t_{wb,in}$), for different values of mass flow rate ratio. Now, as the inlet wet-bulb temperature ($t_{wb,in}$) increases, the outlet process fluid temperature ($t_{p,out}$) increases due to the decreasing difference between the inlet process fluid temperature ($t_{p,in}$) and the inlet wet-bulb temperature ($t_{wb,in}$) keeping in mind that the surface area is constant. Thus, with the inlet process fluid temperature ($t_{p,in}$) as well as its perturbation ($\Delta t_{p,in}$) constant and changes in the outlet process fluid temperature ($\Delta t_{p,out}$) decreasing with the increasing wet-bulb temperature, the
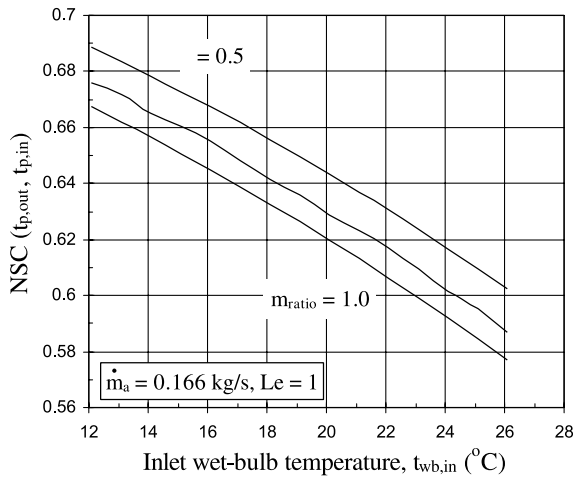
Fig. 6. Variation of process fluid outlet temperature NSC with respect to $t_{p,in}$ as a function of $t_{wb,in}$ and different mass flow rate ratios.

combination of these quantities causes the NSC to decrease. For lower mass flow ratios, the NSC is higher since the steady-state water temperature is higher in the closed circuit that causes the outlet process fluid temperature ($t_{p,out}$) as well as the changes in it ($\Delta t_{p,out}$) to rise.

Similarly, Fig. 7 is the normalized form of the plot between process fluid outlet temperature sensitivity coefficient ($\partial t_{p,out}/\partial t_{p,in}$) versus the inlet process fluid temperature, for different values of mass flow rate ratio. Now, as the inlet process fluid temperature ($t_{p,in}$) increases, the outlet process fluid temperature ($t_{p,out}$) also increases, as the surface area is constant. In this regard, the changes in the outlet process fluid temperature ($\Delta t_{p,out}$) decrease as the steady-state water temperature also rises reducing heat transfer from the
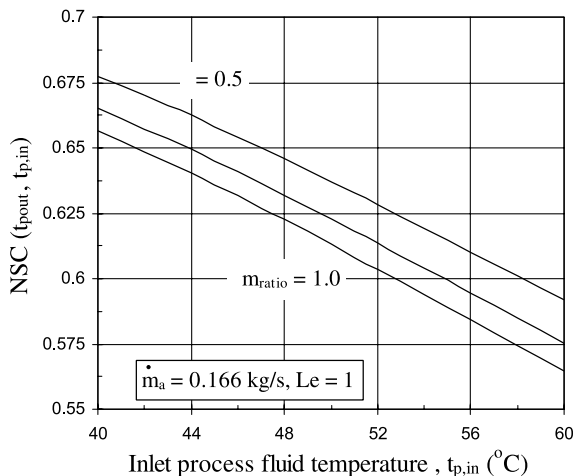

Fig. 7. Variation of process fluid outlet temperature NSC with respect to $t_{p,in}$ as a function of $t_{p,in}$ and different mass flow rate ratios.

process fluid. With the perturbation of the inlet process fluid temperature ($\Delta t_{p,in}$) constant, the combination of these quantities causes the NSC to decrease as the process fluid inlet temperature ($t_{p,in}$) increases. For lower mass flow ratios, the NSC is higher for the reasons as described earlier for Fig. 6.

4. Sensitivity analysis—evaporative condenser

The normalized sensitivity coefficients for the evaporator condenser model discussed in Dreyer [12] and the companion paper [15] are calculated and the results are shown for different mass flow rate ratios. Similar to the evaporative cooler, a preliminary examination of the sensitivity of all variables that included all mass flow rates (air, water and refrigerant) as well as relevant (ambient and refrigerant) temperatures showed that the refrigerant temperature (t_r) had the highest value for the normalized sensitivity coefficient for the response variables investigated. Therefore, variation in the sensitivity values of only this coefficient was shown.

4.1. Design study

Fig. 8 is normalized form of the plot between (surface) area sensitivity coefficient ($\partial A/\partial t_r$) versus the inlet wet-bulb temperature ($t_{wb,in}$), for different values of mass flow rate ratio. Fig. 8 shows that, as the value of the inlet wet-bulb temperature ($t_{wb,in}$) increases, the NSC increases. The condensing temperature (t_r) as well as its perturbation (Δt_r) is constant. As the inlet wet-bulb temperature ($t_{wb,in}$) increases, the decreasing difference between the condensing temperature (t_r) and the inlet wet-bulb temperature ($t_{wb,in}$) gives rise to larger surface area requirements as well as a higher rate of changes in area (ΔA) (refer to Eq. (20) of the companion paper [15]). We notice, again, that there is little effect of different mass flow rate ratio on the sensitivity values. Normalized sensitivity coefficients were also calculated for perturbations in the inlet wet-bulb temperature ($t_{wb,in}$) but the values were much less than 1 for the range investigated, and, thus, it was not shown.

Similarly, Fig. 9 is the normalized form of the plot between (surface) area sensitivity coefficient ($\partial A/\partial t_r$) versus the condensing temperature (t_r), for different values of mass flow rate ratio. We note that, as the value of the condensing temperature (t_r) increases, the NSC decreases and the effect of mass flow rate ratios is negligible. As the condensing temperature (t_r) increases, the heat load decreases, which subsequently requires less surface area and the increasing value of ($t_r - t_{wb,in}$) causes a smaller rate of change in area (ΔA) (refer to Eq. (20) of the companion paper [15]) as well. With the perturbation of the condensing temperature (Δt_r) the same, these factors combine to decrease the NSC as the condensing temperature (t_r) increases.
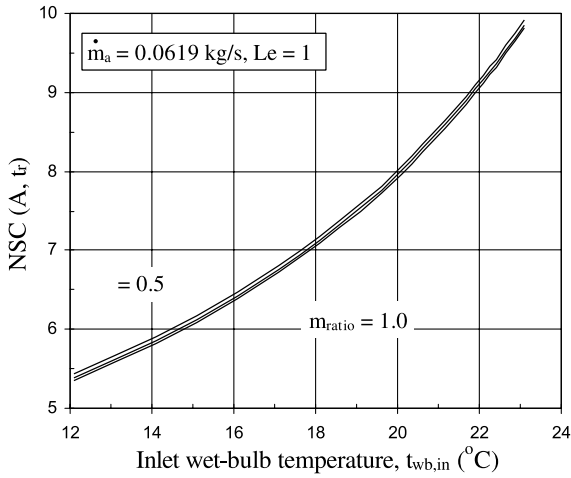
Fig. 8. Variation of area NSC with respect to t_r as a function of $t_{wb,in}$ for different mass flow rate ratios.

4.2. Rating study

Fig. 10 is the normalized form of the plot between effectiveness sensitivity coefficient ($\partial\varepsilon_{ec}/\partial t_r$) versus the inlet wet-bulb temperature ($t_{wb,in}$), for different values of mass flow rate ratio. It shows that, as the inlet wet-bulb temperature ($t_{wb,in}$) increases, the NSC also increases. The condensing temperature as well as its perturbation (Δt_r) is constant. As the inlet wet-bulb temperature ($t_{wb,in}$) increases, the decreasing difference between the condensing temperature (t_r) and the inlet wet-bulb temperature ($t_{wb,in}$) decreases the effectiveness and it becomes more difficult to condense the refrigerant but the change of ($\Delta\varepsilon_{ec}$) increases. The effect of mass flow rate ratios is again seen to be negligible. Normalized sensitivity coefficients were also calculated for perturbations in the refrigerant flow rate ($\dot{m}_r$)

Fig. 10. Variation of effectiveness NSC with respect to t_r as a function of $t_{wb,in}$ for different mass flow rate ratios.

but the values were near to 1 for the range investigated (not shown).

Similarly, Fig. 11 is the normalized form of the plot between effectiveness sensitivity coefficient ($\partial\varepsilon_{ec}/\partial t_r$) versus the condensing temperature (t_r), for different values of mass flow rate ratio. We note from these plots that, as the condensing temperature (t_r) increases, the NSC decreases. The perturbation of the condensing temperature (Δt_r) is constant. As the condensing temperature (t_r) increases, the increasing difference between the condensing temperature (t_r) and the inlet wet-bulb temperature ($t_{wb,in}$) increases the effectiveness as well as the change of ($\Delta\varepsilon_{ec}$) and it becomes easier to condense the refrigerant. The effect of mass flow rate ratios is found to be negligible. Perturbations in the refrigerant flow rate ($\dot{m}_r$) gave near to unitary values for the NSC (not shown).
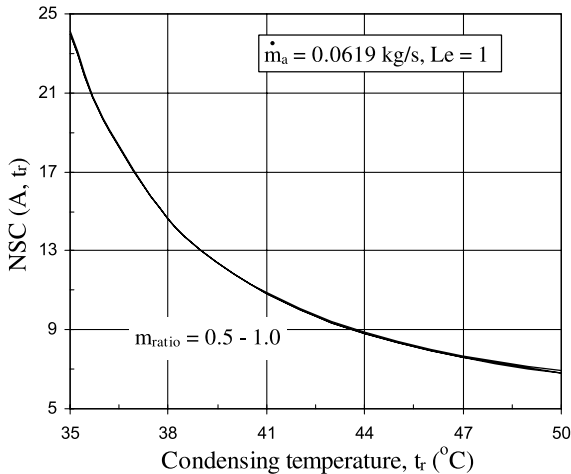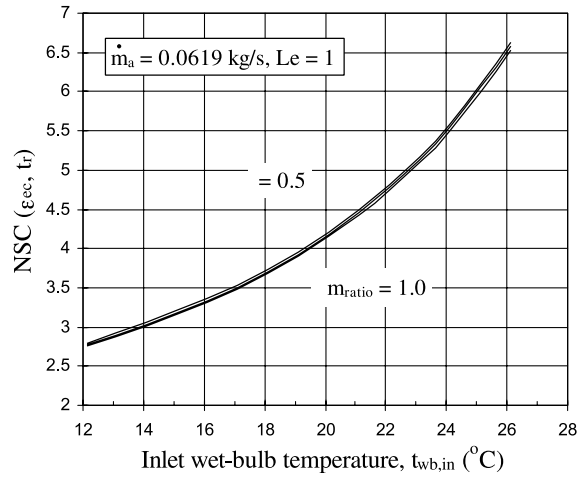

Fig. 9. Variation of area NSC with respect to t_r as a function of t_r for different mass flow rate ratios.
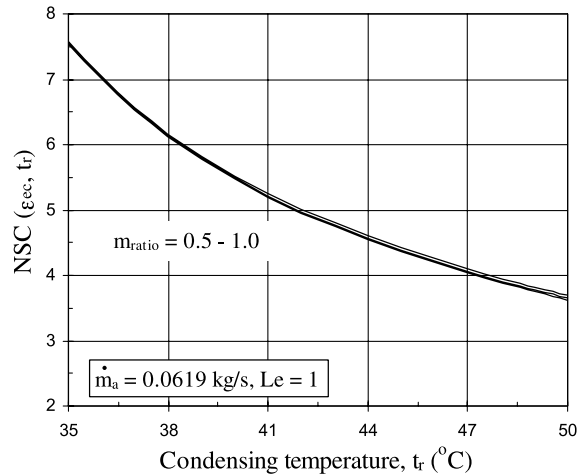

Fig. 11. Variation of effectiveness NSC with respect to t_r as a function of t_r for different mass flow rate ratios.

5. Concluding remarks

The validated mathematical models of evaporative coolers and condensers are used to perform a sensitivity analysis of important response variables. In terms of designing evaporative coolers, the sensitivities are not affected by the value of the mass flow ratio. Furthermore, the surface area (A) is most sensitive to changes in the outlet process fluid temperature ($t_{p,out}$) followed by the inlet process fluid temperature ($t_{p,in}$). Also, a comparison of the influence of both parameters on the response variable, in this case, indicates that it becomes closer to being the same at lower inlet relative humidities and for values of the outlet process fluid temperature ($t_{p,out}$) that are closer to the inlet process fluid temperature ($t_{p,in}$). In rating evaporative coolers, effectiveness is most sensitive to the process fluid flow rate ($\dot{m}_p$) and inlet process fluid temperature ($t_{p,in}$), respectively. Also, the process fluid outlet temperature ($t_{p,out}$) is most sensitive to the process fluid inlet temperature ($t_{p,in}$).

Higher relative humidities at the inlet decrease sensitivity of the response variables investigated. The results are also indicative of the fact that the selection or changes regarding the ambient conditions do not reverse the order of importance with respect to input variables. Regarding evaporative condensers, the plots show that the sensitivities are not affected by the value of the mass flow ratio and that the condensing temperature seems to be the most important factor in design as well as rating. For evaporative condenser design, it was seen that for a 53% increase in the inlet relative humidity, the normalized sensitivity of the response variable increased 1.8 times and, for a 15 °C increase in the condenser temperature, the sensitivity increased by 3.5 times. In performance rating of evaporative condenser, it was noticed that for a 72% increase in the inlet relative humidity, the normalized sensitivity coefficient increased by 2.4 times and, for a 15 °C increase in the condenser temperature, the sensitivity doubled.

Acknowledgements

References

[1] J.E. Kitchell, D.J. Stewart, D. Weininger, Applications of a bioenergetic model to yellow perch (*Perca flavescens*) and walleye (*Stizostedion vitrem vitrem*), J. Fish. Res. Board Can. 34 (1977) 1922–1937.
[2] M. Masi, S. Fogliani, S. Carra, Sensitivity analysis on indium phosphide liquid encapsulated czochralski growth, Cryst. Res. Technol. 34 (9) (1999) 1157–1167.
[3] D. Jamu, R.H. Piedrahita, Aquaculture pond modeling for the analysis of environmental impacts and integration with agriculture: model evaluation and application to the ecological analysis of integrated aquaculture/agriculture systems, PD/A CRSP 17th Annual Technical Report, USA, 2000.
[4] B. Chen, L. Tong, Sensitivity analysis of heat conduction for functionally graded materials, Mater. Des. 25 (2004) 663–672.
[5] C.A. James, R.P. Taylor, B.K. Hodge, The application of uncertainty analysis to cross flow heat exchanger performance predictions, Heat Transfer. Eng. 16 (4) (1995) 50–62.
[6] J.H. Kim, T.W. Simon, Journal of heat transfer policy on reporting uncertainties in experimental measurements and results, ASME J. Heat Transfer. 115 (1) (1993) 5–6.
[7] S.J. Kline, F.A. McClintok, Describing uncertainties in single sample experiments, Mech. Eng. (1953) 3–8.
[8] B.N. Taylor, C.E. Kuyatt, Guidelines for evaluating and expressing the uncertainty of NIST measurement results. National Institute of Standards and Technology Technical Note, 1994. p. 1297.
[9] C.A. James, R.P. Taylor, B.K. Hodge, Analysis and design of energy systems, 3rd ed, Prentice Hall, Englewood Cliffs, NJ, 1998.
[10] X.C. Guo, T.S. Zhao, A parametric study of an indirect evaporative air cooler, Int. Commun. Heat Mass Transfer 25 (1998) 217–226.
[11] W. Zalewski, B. Niezgoda-Zelasko, M. Litwin, Optimization of evaporative fluid coolers, Int. J. Refrig. 23 (2000) 553–565.
[12] A.A. Dreyer, Analysis of evaporative coolers and condenser, MSc Thesis, University of the Stellenbosch, Republic of South Africa, 1988.
[13] R.J. Moffat, Using uncertainty analysis in the planning of an experiment, Trans. ASME J. Fluids Eng. 107 (1985) 173–178.
[14] F. Ardente, G. Beccali, M. Cellura, V. Lo Brano, Life cycle assessment of a solar thermal collector: sensitivity analysis, energy and environmental balances, Renew. Energy 30 (2005) 109–130.
[15] B.A. Qureshi, S.M. Zubair, A comprehensive design and rating study of evaporative coolers and condensers. Part I. Performance evaluation, Int. J. Refrig., this issue.